

# Improved Stability and Targeted Cytotoxicity of Epigallocatechin-3-Gallate Palmitate for Anticancer Therapy

Xuerui Chen,<sup>#</sup> Bingbing Liu,<sup>#</sup> Rongliang Tong, Shiping Ding, Jian Wu, Qunfang Lei,<sup>\*</sup> and Wenjun Fang<sup>\*</sup>



Cite This: *Langmuir* 2021, 37, 969–977



Read Online

ACCESS |



Metrics & More

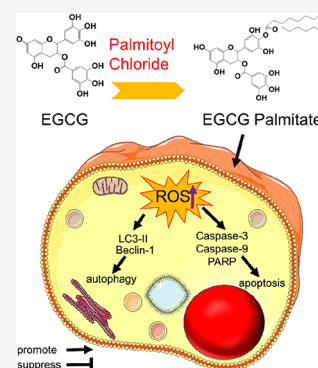


Article Recommendations



Supporting Information

**ABSTRACT:** Although with high antioxidant activity, epigallocatechin-3-gallate (EGCG) was restricted by its poor chemical stability in practical applications. One of EGCG derivatives, EGCG palmitate, was synthesized with EGCG and palmitoyl chloride to overcome instability of EGCG. However, uncertainties still exist in chemical stability and cytotoxicity of EGCG palmitate, which are essential for further exploration in anticancer therapy. Our work aims to analyze the resistance of EGCG palmitate to oxidation and summarize its targeted inhibition efficiency on cancerous cells and normal cells. High-performance liquid chromatography analysis confirmed that EGCG palmitate remained stable in air and Dulbecco's modified eagle medium (DMEM) for a longer time than EGCG. Antioxidative and pro-oxidative effects of EGCG palmitate on treated cells are proposed through reactive oxygen species (ROS) detection, respectively. It reveals that pro-oxidants by H<sub>2</sub>O<sub>2</sub> production can exert antiproliferative and proapoptotic effects on cancerous cells and stimulate autophagy, while an antioxidant relieves oxidative stress caused by superoxide as compared to normal cells. Consequently, targeted cytotoxicity is adopted by EGCG palmitate-treated cancerous cells. Results above manifest that EGCG palmitate possesses potential to serve as a promising prodrug in anticancer treatment.



## 1. INTRODUCTION

Green, white, yellow, oolong, black, or dark tea, beverage derived from *Camellia sinensis*, has incredible health-promoting effects. Their benefits to health are mainly from catechins, and one of the major bioactive polyphenol is (–)-epigallocatechin-3-gallate (EGCG).<sup>1</sup> Indeed, EGCG was found with biological activities, such as neuroprotective, antiatherosclerotic, anti-inflammatory, antidiabetic, antiobesity, and cardioprotective.<sup>2–4</sup> Though scientists attribute the benefits of EGCG to its antioxidant bioactivity, growing evidences imply that pro-oxidant bioactivity of EGCG could induce oxidative stress, thus provoking the inhibition of tumor development.<sup>5,6</sup> For example, EGCG was found to induce oxidative stress and stimulate apoptosis and DNA breaks in human lung cancer H1299 cell xenograft tumors rather than normal tissues.<sup>7</sup> Moreover, pro-oxidant activity that arises from mitochondrial dysfunction can result in ROS-dependent DNA double-strand damages.<sup>8–10</sup> EGCG displays significant pro-oxidant effects, usually under high-dose conditions. The pro-oxidant actions of EGCG play a dual role, being both beneficial and harmful. High doses of EGCG not only cause cytotoxicity in vitro but also result in living body hepatotoxicity, nephrotoxicity, and gastrointestinal disorders. Otherwise, EGCG as antioxidants can change the chromatin of normal cells either by directly affecting the transcription of the DNA backbone or targeting the related proteins through post-translational modifications associated with the apoptosis.<sup>11–13</sup> Both pro-oxidant and

antioxidant bioactivities of EGCG are associated with stimulating apoptosis by disordering DNA transcription, causing the endoplasmic reticulum stress, as well as the early part (LC3-II and beclin-1) and the late phase (LAMP-1) of autophagic pathways.<sup>14–17</sup>

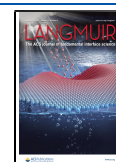
Autophagy is a dynamic cellular pathway to degrade and recycle damaged or aged proteins and organelles. It is close to cancer and probably affects both the promotion and prevention of cancer. Transmission electron microscopy (TEM), Western blotting, and immunofluorescence of LC3 are the most reliable and conventional techniques to evaluate autophagic levels including the LC3 protein and GFP-LC3 fusion. Apart from autophagy, apoptosis is another programmed cell death, which is generally characterized by distinct morphological characteristics and energy-dependent biochemical mechanisms. Flow cytometry and Western blotting have been widely used to analyze apoptosis and apoptosis-marked proteins.

These previous studies demonstrate that EGCG can stimulate autophagy and endoplasmic reticulum stress and

**Received:** December 2, 2020

**Revised:** December 13, 2020

**Published:** January 4, 2021



simultaneously induce apoptosis in cancerous cells.<sup>18</sup> Taken together, EGCG exerts its pharmacological targeted activities in suppressing proliferation of cancerous cells. However, poor chemical stability and rapid decomposition have restricted the utilization of EGCG in chemotherapy.

In this regard, several structural modifications were studied to increase the chemical/metabolic stability of EGCG, wherein palmitoyl chloride with a long fatty acid chain has already been used to synthesize EGCG derivatives.<sup>19,20</sup> According to our previous study, EGCG palmitate has already been synthesized and showed lipophilicity.<sup>21</sup> However, as we all know, the chemical stability and cytotoxicity of EGCG palmitate have not been studied in detail, especially for the pro-oxidant, antioxidant, apoptosis, and autophagy. They can affect the viabilities of cancerous cells and normal cells, respectively, and show potentials of EGCG palmitate in anticancer therapy. Deeper investigations are essential to definitely make sure of the chemical stability and targeted cytotoxicity of EGCG palmitate.

In this work, we aim to confirm EGCG palmitate as an anticancer drug by relevant analysis. The improved structure stability will be demonstrated by the purity changes of EGCG palmitate after it is maintained in physical conditions for several indicated times and compared to that of EGCG in the same conditions. Their targeted cytotoxicity will be compared between cancerous cells and normal cells through their cell viability, antioxidant and pro-oxidant activities, and induction of autophagy and apoptosis. The results above can bring a further study on the anticancer efficiency of EGCG palmitate, thus provide its potential as an anticancer prodrug.

## 2. MATERIALS AND METHODS

**2.1. Materials.** Trypsin/EDTA (EDTA, 0.2 g·L<sup>-1</sup> and trypsin, 1.7 × 10<sup>5</sup> U·L<sup>-1</sup>), dimethyl sulfoxide (DMSO), fetal bovine serum (FBS), Dulbecco's modified eagle medium (DMEM), phosphate buffer saline (PBS), glyceraldehyde-3-phosphate dehydrogenase (GAPDH), and [3-(4,5-dimethylthiazol-2-yl)-2,5-diphenyltetrazolium bromide] (MTT) were purchased from Sigma–Aldrich. EGCG (purity, 95%) was purchased from Pulmeidi. Inc. The Immunology Institute, School of Medicine, Zhejiang University offered HEK 293 cells and HeLa cells.

**2.2. Preparation of EGCG Palmitate.** EGCG palmitate was prepared according to the previous literature.<sup>21</sup> In a typical one-step synthesis protocol, EGCG (4.58 g, 10 mmol) was added to 100 mL of acetone and heated in a 40 °C water bath. Sodium acetate (2.46 g) was added into the solution after being completely dissolved. Palmitoyl chloride (5.49 g, 0.020 mol) was added dropwise to the solution and stirred. The mixture was filtered and washed with 100 mL of deionized water after reacting for 6 h, and 100 mL of ethyl acetate was added to be extracted. The organic phase was washed twice with deionized water, dried with anhydrous sodium sulfate, and concentrated under a reduced pressure.

**2.3. Measurements.** EGCG and EGCG palmitate were analyzed by reversed-phase high performance liquid chromatography (HPLC), which is combined with ultraviolet measurement (1290 VWD) and an Agilent 1290 HPLC unit (Agilent Technologies, U.S.A.). The samples were obtained from a Cosmosil ODS C18 column (4.6 mm × 250 mm, 5 μm; Nacalai Tesque Inc., Japan). Acetonitrile:water:formic acid = 80:20:0.2 (v/v) was the component of eluent A, and acetonitrile:water:formic acid = 10:90:0.2 (v/v) was the component of eluent B. The following gradient program was set as follows: 0–20 min, linear gradient of 0–10% B; 21–60 min, 88% B isocratic. We detected fractions at 275 nm in UV–vis detection with a 1.0 mL/min flow rate. EGCG at 0.009 mM was incubated in 19 mL of DMEM in a tube, and 0.073 mM of EGCG palmitate was placed in a tube with DMEM sonicated by an ultrasound disintegrator for 30 min. At

different time points, 20 μL of the medium was injected into an HPLC system.

**2.4. Cell Culture.** Human embryonic kidney cell 293, referred to as HEK 293 cells, belongs to a specific cell line originally derived from human embryonic kidney cells, which are immortalized and grown in a tissue culture. HEK 293 cells have been widely used as normal cells in biological researches for many years, because of their reliable growth and propensity for transfection. HeLa cells, a cell type in an immortal cell line, are studied as cancerous cells in scientific researches. The cell line was derived from cervical cancer cells.

HEK 293 cells and HeLa cells have been maintained in DMEM in addition with 50 mg·mL<sup>-1</sup> streptomycin, 50 U·mL<sup>-1</sup> penicillin, and 10% FBS. These cells were cultured at 37 °C in a humidified 5% CO<sub>2</sub> atmosphere.

**2.5. MTT Analyses.** We seeded HEK 293 cells (8 × 10<sup>4</sup> cells per well) or HeLa cells (1 × 10<sup>5</sup> cells 1 × 10<sup>5</sup> cells) into 96-well plates, 12 h before. Then, we replaced the medium with DMEM on a series of concentrations of EGCG or EGCG palmitate without FBS for indicated times before adding a 0.5 mg × mL<sup>-1</sup> MTT (100 μL) solution for 4 h. Finally, we introduced DMSO (100 μL) into a tested well of the 96-well plate and measured the absorbance at 570 nm.<sup>22</sup>

**2.6. Cellular Uptake of EGCG and EGCG Palmitate.** Cellular uptakes of EGCG and EGCG palmitate were examined under confocal laser scanning microscopy (CLSM) (Zeiss Lsm710nlo). The green fluorescent dye (FITC) was used to label the EGCG or EGCG palmitate, and LysoTracker Red probes were used to detect lysosomes. Visualizations of EGCG and EGCG palmitate in HeLa cells were determined by the fluorescence. HeLa cells were seeded onto glass slides in the six-well plates and grown in a humidified chamber (37 °C and 5% CO<sub>2</sub>). Cells were treated with EGCG and EGCG palmitate for different time intervals (2 and 4 h). After treatments, the cells were fixed on slides with 4% paraformaldehyde (PFA) for 10 min at RT. The slides were quickly covered with a cover slip, and then monitored using CLSM.

**2.7. Evaluation of ROS Levels.** We applied dichlorofluorescein diacetate (DCFH-DA) to evaluate ROS levels. Then, we cultured HEK 293 cells (8 × 10<sup>5</sup>) or HeLa cells (1.0 × 10<sup>6</sup>) into a six-well plate before 12 h and incubated them with the drug for 24 h. Next, we trypsinized the cells and incubated them with DCFH-DA (10 mmol/L) for 15 min at 37 °C. Finally, we analyzed the cells under a flow cytometer after washed with PBS twice.

We cultured HEK 293 cells (8 × 10<sup>5</sup>) or HeLa cells (1.0 × 10<sup>6</sup>) into a six-well plate before 12 h and incubated them with 100 μmol/L H<sub>2</sub>O<sub>2</sub> for 2 h before drug treatment for 24 h. Next, we trypsinized cells and incubated them with DCFH-DA (10 mmol/L) for 15 min at 37 °C. Finally, we analyzed the cells under a flow cytometer after washed with PBS twice.

**2.8. Detection of Apoptosis.** We utilized an Annexin-V apoptosis kit (Bingyuntian, China) to measure apoptosis. HEK 293 cells or HeLa cells were incubated with EGCG or EGCG palmitate at a definite concentration. After 24 h, we trypsinized these cells and washed them twice with PBS. Next, we suspended cells in a 1X Annexin-V binding buffer (200 μL) with Annexin-V-FITC (5 μL) alone or combined with PI (10 μL). Finally, the cells were maintained at 37 °C for 15 min and analyzed by flow cytometry.

**2.9. Observation of Autophagic Flux.** Based on a manufacturer protocol, we used mRFP-GFP-LC3 (adenovirus; Hanheng, China) to transfect HEK 293 cells or HeLa cells. After the treatment of EGCG or EGCG palmitate for 12 h, cells with green fluorescence and red fluorescence were observed under CLSM (Zeiss Lsm710nlo).

**2.10. Observation of MDC-Stained Autophagic Vacuoles.** We used dansylcadaverine (MDC), fluorescent dye, to stain autophagic vacuoles. First, we seeded HEK 293 cells or HeLa cells in 24-well plates before 12 h. After treating the cells with drugs for 24 h, we stained the cells using MDC (0.05 mmol·L<sup>-1</sup>) at 37 °C for 10 min. Finally, we washed them twice using PBS and detected autophagic vacuoles under CLSM (Zeiss Lsm710nlo).

**2.11. Observation of Autophagosomes.** We used TEM to observe autophagosomes. First, we collected HEK 293 cells or HeLa cells and washed them twice with PBS after 24 h of EGCG or EGCG

palmitate treatment. Then, we fixed these cells with a pH 7.4 solution containing glutaraldehyde (2.5%) and paraformaldehyde (2.0%) overnight. Next, we put the cell samples into OsO<sub>4</sub> (1%) for 30 min. Finally, we could observe autophagosomes under TEM (JEM-1200EX, JEOL, Japan).

**2.12. Expression of Autophagic and Apoptotic Proteins by Western Blotting.** We used a general protein extraction reagent (Biotek, China) in addition with a protease inhibitor (1.0%) to extract cell proteins and used SDS-PAGE (12%) to separate them. Then, we utilized electrophoresis to transfer the cell proteins to polyvinyl difluoride membranes (0.45 μmol·L<sup>-1</sup>). The antibodies we used are at a 1:1000 dilution ratio and as follows: LC3(4108), beclin-1(ab62557), poly(ADP-ribose) polymerase (PARP) (ab194586), caspase-9(ab2013) and caspase-3(ab90437), and GAPDH (ab181602). Finally, we developed the membrane with an Immobilon Western Chemiluminescent HRP substrate (Millipore).

**2.13. Statistical Analysis.** We replicated every experiment twice and analyzed three samples per replicate (*n* = 3). The results were presented as mean ± SD of three values. The level for the accepted statistical significance was *P* < 0.05.

### 3. RESULTS AND DISCUSSIONS

**3.1. Chemical Stability of EGCG Palmitate.** Previous studies of the catechin structure–activity relationship have demonstrated that the antioxidative abilities of EGCG could be ascribed to the presence of dihydroxy and trihydroxy groups in three rings of EGCG. Under normal physiological conditions (pH 7.4, 37 °C), EGCG is auto-oxidized and converted to *o*-quinone through nonenzymatical dehydrogenation of phenolic hydroxyl groups. Based on the chemical structure of EGCG, EGCG palmitate is synthesized with EGCG and palmitoyl chloride to have a long carbon chain. Its structure is determined by <sup>1</sup>H and <sup>13</sup>C NMR in our previous study.<sup>21</sup> The peak at 2800–3000 cm<sup>-1</sup> in the FTIR spectrum of EGCG palmitate refers to the presences of –CH<sub>3</sub> and –CH<sub>2</sub>–. The peak at 3384 cm<sup>-1</sup> in the FTIR spectrum of EGCG palmitate refers to the ester group of EGCG palmitate and verifies its palmitate hydroxyl group (Figure S1a). The FTIR spectrum above reveals that EGCG palmitate has a long carbon chain and confirms that EGCG palmitate is 4'-*O*-palmitoyl EGCG (Figure 1). The thermostability was recorded by TGA with an increasing temperature under a nitrogen gas flow. It shows a

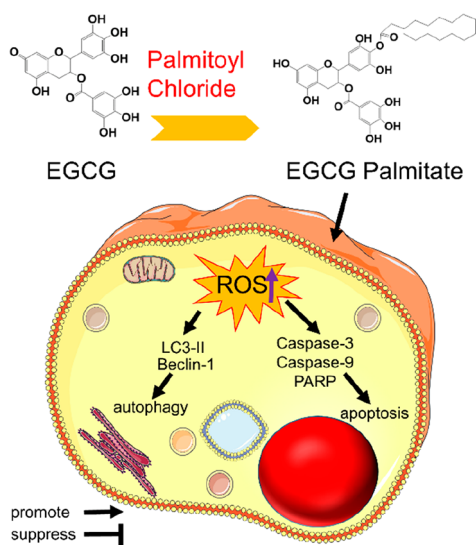


**Figure 1.** Schematic illustration of EGCG palmitate with targeted cytotoxicity.

two-step mass loss in the thermogram of EGCG, which is resulted from evaporation of H<sub>2</sub>O (80 °C) and chemical structure degradation (254 °C). EGCG palmitate exhibits a three-step mass loss, whose stages are resulted from evaporation of H<sub>2</sub>O, thermal degradation (200 °C), and decomposition of the acetylated and deacetylated units of the palmitate (Figure S1b).

Stability of EGCG palmitate was further evaluated by HPLC to compare retentions of EGCG palmitate and EGCG stored in air or dissolved in a culture medium (DMEM) for some indicated times. Storage temperature and conditions were considered as important factors for the protection of polyphenols.<sup>23,24</sup> The samples stored in air at 25 and –20 °C for several days are shown in Figure 2. Generally, the retention of EGCG palmitate and EGCG decreased while the storage temperature increased from –20 to 25 °C. They tended to form their oligomers at lower storage temperatures, which might lead to their diversity of bioactive retention; thus, detailed quantification was analyzed by HPLC. An amount of 80.5% EGCG palmitate was left after stored for 60 days, while 60.0% EGCG was left after stored for 60 days at 25 °C (Figure 2b). An amount of 74.8% EGCG palmitate was left after stored for 150 days at –20 °C, and 63.5% EGCG was left after stored for 150 days at –20 °C. Consistently, EGCG palmitate is more stable than EGCG when stored in air at 25 and –20 °C.

Furthermore, bioactive retentions of EGCG palmitate and EGCG dissolved in DMEM for some indicated times were measured due to the fact that DMEM mimics the body fluid with a pH value around 8 at 37 °C. EGCG dissolved in DMEM degraded quickly with only 15.9% of retention within 1 h and none left within 3 h, which indicates fast degradation of EGCG in the DMEM. As for EGCG palmitate, its long fatty acid chain degraded within 1 h. EGCG palmitate was transformed into EGCG and 3.1% was left after 3 h, during which the retention time of EGCG palmitate in physiological conditions was prolonged. As seen in Figure 2a, EGCG palmitate kept a slower speed of degradation in DMEM than EGCG. The longer retention times of EGCG palmitate whether exposed in air or dissolved in DMEM imply that EGCG palmitate has improved antioxidant stability regardless of different conditions.

**3.2. Intracellular ROS Levels Affected by an Anti-oxidant or Pro-oxidant.** Previous studies reported that effects of EGCG on cancerous cells and normal cells depended on the role that the pro-oxidant or antioxidant are playing in the experimental conditions.<sup>25,26</sup> It has shown both prophylactic and therapeutic efficacy in multiple human cancers. The pro-oxidant effect of EGCG was considered as a potential mechanism for anticancer action. EGCG could yield superoxide anion radicals (O<sub>2</sub><sup>-</sup>) and EGCG radicals (EGCG) when oxidized in cells. O<sub>2</sub><sup>-</sup> could also form substantial amounts of H<sub>2</sub>O<sub>2</sub> via the disproportionation reaction.<sup>27</sup> One EGCG molecule could produce more than two H<sub>2</sub>O<sub>2</sub> molecules in PBS of neutral pH. H<sub>2</sub>O<sub>2</sub>, singlet oxygen, hydroxyl radicals, superoxide, and peroxides consist of ROS. Thus, EGCG mainly affects the ROS levels through the H<sub>2</sub>O<sub>2</sub> yield. Scientists particularly studied EGCG-mediated ROS production in cancerous cells compared with normal cells and found that EGCG induced differential mitochondrial dysfunction and oxidative stress in normal and cancerous cells.<sup>28</sup> Differential inducibility of ROS and preferential expression of apoptosis-related genes further induced the selectivity of apoptosis in cancer cells. It suggested that cancer cells are more sensitive to

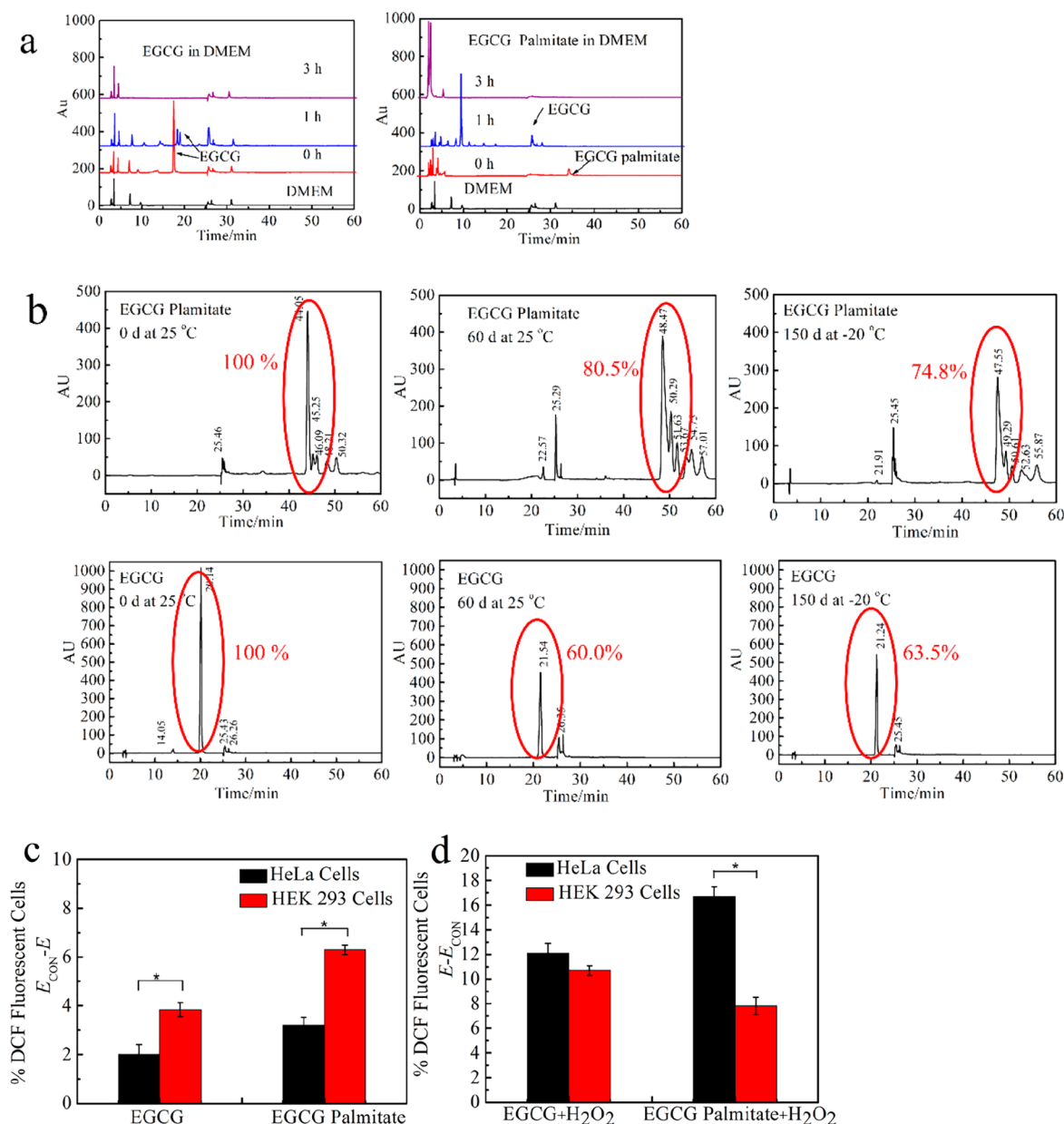


**Figure 2.** (a) Stabilities of EGCG and EGCG palmitate dissolved in DMEM determined by HPLC; (b) stabilities of EGCG palmitate and EGCG in air determined by HPLC; (c) ROS generation detected by flow cytometry for HeLa cells and HEK 293 cells incubated with EGCG or EGCG palmitate ( $250 \mu\text{g}\cdot\text{mL}^{-1}$ ); (d) ROS generation detected by flow cytometry for HeLa cells and HEK 293 cells incubated with EGCG or EGCG palmitate and  $\text{H}_2\text{O}_2$  ( $160 \mu\text{g}\cdot\text{mL}^{-1}$ ). \* $P < 0.05$ .

EGCG than normal cells, and ROS might be selectively toxic to cancer cells.<sup>29</sup>

Hypothetically, EGCG palmitate has similarly prooxidative or antioxidative influence on intracellular ROS levels through  $\text{H}_2\text{O}_2$  regulation when treating cancerous cells and normal cells. According to the above hypothesis, we emphatically analyse its effects on  $\text{H}_2\text{O}_2$  production, which is usually detected by DCFH-DA probe. This probe can be hydrolysed by esterases to the carboxylate anion (DCFH), which is easily oxidated by ROS to form DCF with green fluorescence and observed under flow cytometry. We first evaluated basal ROS level in HEK 293 cells and HeLa cells treated with EGCG palmitate while setting EGCG as reference.<sup>30,31</sup> Intracellular ROS amounts in HeLa cells (cancerous cells) are considerably higher (50%) than those in HEK 293 cells (normal cells),

which indicates EGCG palmitate induces important  $\text{H}_2\text{O}_2$  increment in the cytosol of cancerous cells, as compared to normal cells ( $p < 0.05$ , Figure 2c). One possible supposition is that cancerous cells may be more susceptible to oxidative stress, since their increased growth rate and metabolism cause a heightened basal ROS level.

Then, we would like to figure out whether EGCG palmitate could relieve oxidative stress by decreasing high ROS levels. We pretreated cancerous cells and normal cells with  $\text{H}_2\text{O}_2$  before treating them with an equal dose of EGCG and EGCG palmitate. We found that ROS levels of  $\text{H}_2\text{O}_2$ -pretreated cells were significantly decreased by EGCG palmitate and EGCG treatment, wherein the ROS differences of HeLa cells and HEK 293 cells treated with EGCG palmitate are more remarkable than those treated with EGCG. These results

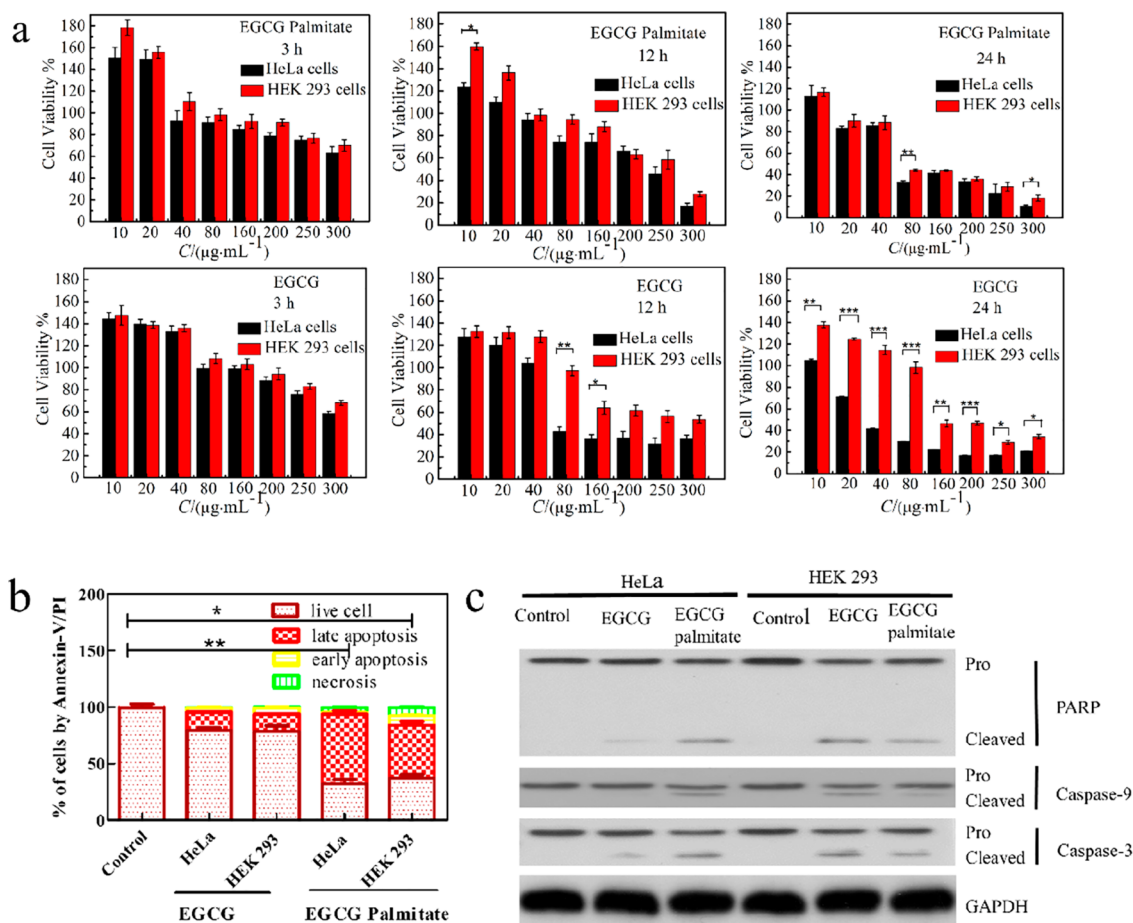


**Figure 3.** (a) Cell viabilities of HeLa cells and HEK 293 cells exposed to EGCG palmitate or EGCG determined by MTT assays; (b) detection of apoptosis using annexin V/PI in HeLa cells or HEK 293 cells treated with EGCG or EGCG palmitate ( $250 \mu\text{g}\cdot\text{mL}^{-1}$ ); (c) PARP, caspase-9, and caspase-3 assayed by the Western blotting analysis on HeLa cells or HEK 293 cells treated with EGCG or EGCG palmitate ( $250 \mu\text{g}\cdot\text{mL}^{-1}$ ) for 12 h; \* $P < 0.05$ ; \*\* $P < 0.01$ ; \*\*\* $P < 0.001$ .

show that the  $\text{H}_2\text{O}_2$  scavenging activity of EGCG palmitate is higher than that of EGCG at an equivalent dose. ROS levels of HEK 293 cells were significantly lower than those of HeLa cells, which suggested a protective function of EGCG palmitate for normal cells in this work ( $p < 0.05$ ). These findings also reveal remarkable bioactivities of EGCG palmitate in healthcare, similar to that of EGCG, which is found to induce dose-dependent oxidative stress in cancerous cells but not normal cells. EGCG palmitate works as a healthcare product with antioxidant bioactivity for normal cells while working as an anticancer drug with pro-oxidative bioactivity for cancerous cells. We conclude that EGCG palmitate has selective cytotoxicity against cancerous cells by favoring to increase the oxidative stress of cancerous cells, thus rendering targeted modulation of ROS levels for cancerous cells.

### 3.3. Effects of EGCG Palmitate on Cell Proliferation.

ROS regulation is associated with induction of apoptosis, necrosis, and autophagy through destroying intracellular substances including lipid membranes, protein, and DNA.<sup>32,33</sup> Before investigating the proliferation of HeLa cells and HEK 293 cells, we first observed cellular penetrations of EGCG and EGCG palmitate at different time intervals (2 and 4 h) under CLSM. The merged images in Figure 4c,d included lysosome- and FITC-labeled EGCG palmitate or EGCG with red and green colors, respectively. The data indicate that EGCG and EGCG palmitate penetrate the cells efficiently and

are mostly localized in the cytoplasmic compartments of the cells. However, intracellular distributions of EGCG palmitate molecules are homogenous and do not change considerably over 4 h compared to EGCG. It can be concluded that EGCG palmitate molecules are stable inside of the cell.

To examine targeted anti-proliferative functions of EGCG palmitate caused by ROS elevation, normal cells and cancerous cells were treated with diverse dosages of EGCG palmitate either for 3, 12, or 24 h. The cell proliferative capacity was inhibited after EGCG or EGCG palmitate treatment in both dose- and time-dependent fashions. In a shorter incubation time (3 h), viabilities of two kinds of cells treated with EGCG are higher than those of cells treated with EGCG palmitate, with their concentration ranging from 40–200  $\mu\text{g}\cdot\text{mL}^{-1}$ . In a longer incubation time (12 and 24 h), EGCG shows a more obvious difference on both HeLa cells and HEK 293 cells, as compared to EGCG palmitate. For example, growth of HeLa cells was inhibited by 30–75% after the 24 h treatment with 20–250  $\mu\text{g}\cdot\text{mL}^{-1}$  of EGCG; the antiproliferative effect of EGCG (20–250  $\mu\text{g}\cdot\text{mL}^{-1}$ ) on HeLa cells was higher, as compared to that on HEK 293 cells at 24 h ( $P < 0.05$ ). The increasing treatment time of EGCG palmitate to 12 and 24 h resulted in a small percentage (2%) of necrotic cells at a concentration of 10  $\mu\text{g}\cdot\text{mL}^{-1}$ . Its  $\text{IC}_{50}$  values for HEK 293 cells and HeLa cells were calculated as  $280.5 \pm 47.2$  and  $220.3 \pm 12.1 \mu\text{g}\cdot\text{mL}^{-1}$ , respectively (Figure 3a). More importantly,

both EGCG and EGCG palmitate show similar tendency of cytotoxicity toward HeLa cells and HEK 293 cells ( $P < 0.05$ ). At higher concentrations ( $80 \mu\text{g}\cdot\text{mL}^{-1}$ ), 24 h of incubation with EGCG palmitate increases the percentage of necrotic HeLa cells up to 50% compared to that of HEK 293 cells, wherein similar phenomena exist among EGCG ( $10\text{--}300 \mu\text{g}\cdot\text{mL}^{-1}$ ). It shows that the proliferation of cancerous cells can be potentially inhibited by EGCG palmitate, in particular, for HeLa cells.

### 3.4. Apoptosis of Cells Treated with EGCG Palmitate.

Cellular ROS accumulation in cancerous cells was recognized as important intermediates in activating the apoptosis process. Cell apoptosis could be triggered by either the intrinsic mitochondrial pathway or the external death receptor pathway. The mitochondrial pathway could be induced by intracellular stresses, such as oxidative stress. Our investigations would determine whether EGCG palmitate can induce targeted apoptosis of cancerous cells.<sup>34</sup> Proapoptotic effects of EGCG palmitate were studied after 12 h of incubation by double staining of PI and Annexin V-FITC, which were revealed by the percentage of late apoptotic cells (PI+ and Annexin V-FITC+) and early apoptotic cells (PI- and Annexin V-FITC+). The percentage of late and early apoptotic features in HEK 293 cells treated with EGCG palmitate is 55.52% and is less than in HeLa cells (63.61%) with the treatment of EGCG palmitate (Figure 3b). EGCG palmitate was found to induce relatively more apoptotic and necrotic cell death in cancerous cells as compared to normal cells in this work. They are resulted from excessive production of ROS caused by the pro-oxidant.

Next, the Western blotting assay was used to evaluate several marker proteins of apoptosis, such as PARP, caspase-3, and caspase-9, for an insight in the apoptotic pathways involved (Figure 3c). PARP overexpression is caused by numerous cellular stress factors, and cleaved PARP represents a hallmark of apoptosis. We noticed differences in the activity of both PARP and cleaved PARP between normal and cancerous cells 12 h after EGCG palmitate treatment, while the signal between EGCG and EGCG palmitate was equal. In the caspase family, the most important regulators of apoptosis are caspase-3 and caspase-9, executioner caspases, which are inactive dimers, the activation of which is launched by proteolytic cleavage of a certain subunit. Different proteases cleave the caspase-3 and caspase-9 zymogens to activate them (cleaved-caspase-3 and cleaved-caspase-9). The cleaved substrates lead to alterations in the protein function and cellular changes related to apoptosis. Caspase-9 and caspase-3 were found to have additional two bands for procaspase and cleaved-caspase, demonstrating that apoptosis is activated under EGCG and EGCG palmitate treatments. As compared to HEK 293 cells, EGCG palmitate upregulated proapoptosis-relevant proteins of HeLa cells. Therefore, EGCG palmitate activates apoptosis through a caspase-dependent pathway and has targeted apoptosis induction for cancerous cells.

### 3.5. Autophagy Induced by EGCG Palmitate.

The above results implied participation of elevated ROS in EGCG palmitate-stimulated apoptosis. Nevertheless, it was equally important to evaluate ROS-induced autophagy. TEM was employed to demonstrate the ultrastructures present in cells treated with EGCG palmitate. In Figure 4a, cytoplasmic vacuoles with double-membrane and encapsulated organelles are detected in EGCG palmitate-incubated cells, implying some metabolite degradation in autophagosomes. In addition,

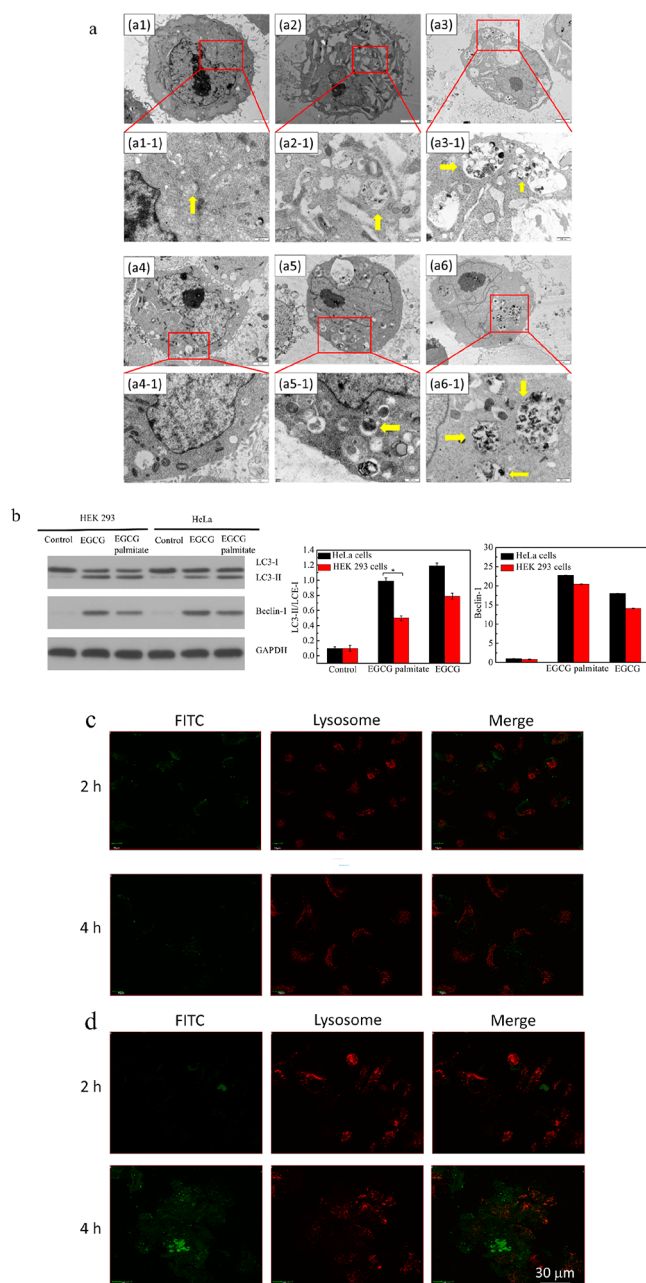


**Figure 4.** (a) TEM images of HeLa cells (a1–a3) and HEK 293 cells (a4–a6) treated with EGCG or EGCG palmitate ( $250 \mu\text{g}\cdot\text{mL}^{-1}$ ) for 12 h. The inset is an enlarged image of the area marked by the square showing individual autophagosomes (yellow arrows). ((a1, a4) control, (a2, a5) EGCG, and (a3, a6) EGCG palmitate). (b) LC3 lipidation and beclin-1 assayed by Western blotting analysis on HeLa cells or HEK 293 cells treated with EGCG or EGCG palmitate ( $250 \mu\text{g}\cdot\text{mL}^{-1}$ ) for 12 h; cellular uptake of (c) EGCG palmitate and (d) EGCG with a  $250 \mu\text{g}\cdot\text{mL}^{-1}$  concentration for HeLa cells.

there are more vacuoles and disappearing organelles in EGCG palmitate-treated HeLa cells, as compared to HEK 293 cells (Figure 4a). These results showed that EGCG palmitate strongly led to cellular damage and autophagosome formation in cancerous cells.

The Western blotting analysis further investigated the expression of autophagic proteins in HEK 293 cells and HeLa cells. EGCG palmitate and EGCG could induce the formation of autophagic vesicles along with the increased

expression levels of LC3-II and beclin-1. More significant changes in the conversion of LC3-I to LC3-II and expression of beclin-1 can be observed in HeLa cells than in HEK 293 cells under the treatment of EGCG palmitate (Figure 4b). These transformations of autophagic proteins demonstrate that autophagy could be stimulated by EGCG palmitate, effectively for cancerous cells.

Then, autophagy flux, a dynamic process of autophagy, labeled by mRFP-GFP-LC3 adenovirus was observed under CLSM. A previous study has divided autophagy flux into three steps: autophagosome formation, autolysosome formation via lysosome–autophagosome fusion, and lysosomal degradation.<sup>35,36</sup> Yellow spot (autophagosomes) and red spot (autolysosomes) formations in mRFP-GFP-LC3 transfected cells can be normalized to determine autophagic flux (Figure 5a). Compared with HEK 293 cells treated with EGCG

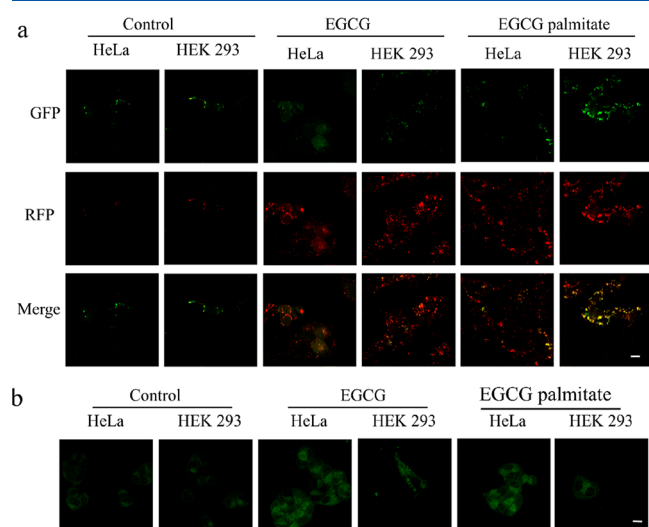


**Figure 5.** (a) Autophagic flux of mRFP-GFP-LC3 transfected cells after incubation with EGCG or EGCG palmitate ( $250 \mu\text{g}\cdot\text{mL}^{-1}$ ) for 24 h (autophagosomes: mRFP+/GFP+ yellow puncta; autolysosomes: mRFP+/GFP-); (b) autophagic vesicles in HeLa cells and HEK 293 cells incubated with EGCG or EGCG palmitate ( $250 \mu\text{g}\cdot\text{mL}^{-1}$ ) from an MDC staining assay observed under CLSM (scale bar,  $20 \mu\text{m}$ ).

palmitate, HeLa cells treated with EGCG palmitate show higher ratios of red:yellow puncta, which indicates that most autophagosomes in HeLa cells were transformed into autolysosomes. We observed EGCG palmitate-boosted autophagic flux by influencing the autophagosome initiation as well as the autophagosome maturation, in particular, for cancerous cells. At the same time, MDC works as probes of autophagy vacuoles, showing the autophagy intensity of cells treated with EGCG palmitate and EGCG by its fluorescence intensity in Figure 5b.<sup>37</sup> HEK 293 cells with the treatment of EGCG palmitate have relatively lower fluorescence intensity as compared to HeLa cells. They are consistent with the conclusion that EGCG palmitate can induce autophagy, especially for cancerous cells.

#### 4. CONCLUSION

In this work, EGCG palmitate was confirmed with improved stability and targeted cytotoxicity for cancerous cells, measured by HPLC, a flow cytometer, CLSM, TEM, MTT analysis, and Western blotting assay. The improved antioxidant stability of

EGCG palmitate was indicated by its lesser losses than that of EGCG under the same conditions. Cancerous cells exposed to EGCG palmitate showed a lower proliferation ratio, increased number of autophagosomes, as well as overexpression of autophagic and apoptotic proteins compared to normal cells, which revealed that EGCG palmitate promoted apoptosis and autophagy in cancerous cells. Oxidative stress in normal cells could be largely decreased by EGCG palmitate, which demonstrates a protective function of EGCG palmitate for normal cells. Therefore, EGCG palmitate works as a healthcare product with antioxidant bioactivity for normal cells while working as an anticancer drug with pro-oxidative bioactivity for cancerous cells. With improved chemical stability and targeted cytotoxicity for cancerous cells, EGCG palmitate has been discovered as a promising anticancer drug candidate.

#### ■ ASSOCIATED CONTENT

##### Supporting Information

The Supporting Information is available free of charge at <https://pubs.acs.org/doi/10.1021/acs.langmuir.0c03449>.

IR spectra for EGCG and EGCG palmitate; TGA curves for EGCG and EGCG palmitate (PDF)

#### ■ AUTHOR INFORMATION

##### Corresponding Authors

Qunfang Lei – Department of Chemistry, Zhejiang University, Hangzhou 310027, China; Phone: +86 571 88208913; Email: [qflei@zju.edu.cn](mailto:qflei@zju.edu.cn); Fax: +86-571-88208913

Wenjun Fang – Department of Chemistry, Zhejiang University, Hangzhou 310027, China; [orcid.org/0000-0002-5610-1623](https://orcid.org/0000-0002-5610-1623); Phone: +86 571 88981416; Email: [fwjun@zju.edu.cn](mailto:fwjun@zju.edu.cn); Fax: +86-571-88981416

##### Authors

Xuerui Chen – Department of Chemistry, Zhejiang University, Hangzhou 310027, China; School of Medicine, Shanghai University, Shanghai 200444, China

Bingbing Liu – Department of Chemistry, Zhejiang University, Hangzhou 310027, China

Rongliang Tong – Division of Hepatobiliary and Pancreatic Surgery, Department of Surgery, First Affiliated Hospital, School of Medicine, Zhejiang University, Hangzhou 310003, China

Shiying Ding – The National Education Base for Basic Medical Sciences, Zhejiang University School of Medicine, Zhejiang University, Hangzhou 310058, China

Jian Wu – Division of Hepatobiliary and Pancreatic Surgery, Department of Surgery, First Affiliated Hospital, School of Medicine, Zhejiang University, Hangzhou 310003, China

Complete contact information is available at: <https://pubs.acs.org/10.1021/acs.langmuir.0c03449>

##### Author Contributions

#X.C. and B.L. contributed equally as first authors.

##### Notes

The authors declare no competing financial interest.

#### ■ ACKNOWLEDGMENTS

This work was supported by the National Natural Science Foundation of China (grant numbers 22003038 and 21473157), the Science Technology Department of Zhejiang Province (grant number 2015C03034), and the National Key

Research and Development Program of China (grant number 2017YFF0211002).

## REFERENCES

- (1) Esmaeelpanah, E.; Razavi, B. M.; Hasani, F. V.; Hosseinzadeh, H. Evaluation of epigallocatechin gallate and epicatechin gallate effects on acrylamide-induced neurotoxicity in rats and cytotoxicity in PC 12 cells. *Drug Chem. Toxicol.* **2018**, *41*, 441–448.
- (2) Cao, Y.; Ai, N.; True, A. D.; Xiong, Y. L. Effects of (–)-epigallocatechin-3-gallate incorporation on the physicochemical and oxidative stability of myofibrillar protein–soybean oil emulsions. *Food Chem.* **2018**, *245*, 439–445.
- (3) Colon, M.; Nerín, C. Synergistic, antagonistic and additive interactions of green tea polyphenols. *Eur. Food Res. Technol.* **2016**, *242*, 211–220.
- (4) Chakrabarty, S.; Nag, D.; Ganguli, A.; Das, A.; Dastidar, D. G.; Chakrabarti, G. Theaflavin and epigallocatechin-3-gallate synergistically induce apoptosis through inhibition of PI3K/Akt signaling upon depolymerizing microtubules in HeLa cells. *J. Cell. Biochem.* **2019**, *120*, 5987–6003.
- (5) Fan, Y.-C.; Chan, W.-H. Epigallocatechin gallate induces embryonic toxicity in mouse blastocysts through apoptosis. *Drug Chem. Toxicol.* **2014**, *37*, 247–254.
- (6) Tao, L.; Park, J.-Y.; Lambert, J. D. Differential prooxidative effects of the green tea polyphenol, (–)-epigallocatechin-3-gallate, in normal and oral cancer cells are related to differences in siruin 3 signaling. *Mol. Nutr. Food Res.* **2015**, *59*, 203–211.
- (7) Li, G.-X.; Chen, Y.-K.; Hou, Z.; Xiao, H.; Jin, H.; Lu, G.; Lee, M.-J.; Liu, B.; Guan, F.; Yang, Z.; Yu, A.; Yang, C. S. Pro-oxidative activities and dose-response relationship of (–)-epigallocatechin-3-gallate in the inhibition of lung cancer cell growth: a comparative study *in vivo* and *in vitro*. *Carcinogenesis* **2010**, *31*, 902–910.
- (8) Pawlowska, E.; Szczepanska, J.; Blasiak, J. Pro- and Antioxidant Effects of Vitamin C in Cancer in correspondence to Its Dietary and Pharmacological Concentrations. *Oxid. Med. Cell. Longevity* **2019**, *2019*, 7286737.
- (9) Zan, L.; Chen, Q.; Zhang, L.; Li, X. Epigallocatechin gallate (EGCG) suppresses growth and tumorigenicity in breast cancer cells by downregulation of miR-25. *Bioengineered* **2019**, *10*, 374–382.
- (10) Gbenga-Fabusiwa, F. J.; Oladele, E. P.; Oboh, G.; Adefegha, S. A.; Oshodi, A. A. Polyphenol contents and antioxidants activities of biscuits produced from ginger-enriched pigeon pea-wheat composite flour blends. *J. Food Biochem.* **2018**, *42*, No. e12526.
- (11) Tolouei, S. E. L.; Traesel, G. K.; de Lima, F. F.; de Araújo, F. H. S.; Lescano, C. H.; Cardoso, C. A. L.; Oesterreich, S. A.; do Carmo Vieira, M. Cytotoxic, genotoxic and mutagenic evaluation of *Alibertia edulis* (rich.) a. Rich. ex DC: an indigenous species from Brazil. *Drug Chem. Toxicol.* **2020**, *43*, 200–207.
- (12) Zhang, W.; Zhang, W.; Sun, L.; Xiang, L.; Lai, X.; Li, Q.; Sun, S. The effects and mechanisms of epigallocatechin-3-gallate on reversing multidrug resistance in cancer. *Trends Food Sci. Technol.* **2019**, *93*, 221–233.
- (13) Agunloye, O. M.; Oboh, G. Caffeic acid and chlorogenic acid: Evaluation of antioxidant effect and inhibition of key enzymes linked with hypertension. *J. Food Biochem.* **2018**, *42*, No. e12541.
- (14) Zheng, Q.; Li, W.; Zhang, H.; Gao, X.; Tan, S. Optimizing synchronous extraction and antioxidant activity evaluation of polyphenols and polysaccharides from Ya'an Tibetan tea (*Camellia sinensis*). *Food Sci. Nutr.* **2020**, *8*, 489–499.
- (15) Man, S.; Wang, H.; Zhou, J.; Lu, Y.; Su, Y.; Ma, L. Cardiac Glycoside Compound Isolated from *Helleborus thibetanus* Franch Displays Potent Toxicity against HeLa Cervical Carcinoma Cells through ROS-Independent Autophagy. *Chem. Res. Toxicol.* **2019**, *32*, 2479–2487.
- (16) Marelli, M. M.; Marzagalli, M.; Fontana, F.; Raimondi, M.; Moretti, R. M.; Limonta, P. Anticancer properties of tocotrienols: A review of cellular mechanisms and molecular targets. *J. Cell. Physiol.* **2019**, *234*, 1147–1164.
- (17) Chen, X.; Tong, R.; Shi, Z.; Yang, B.; Liu, H.; Ding, S.; Wang, X.; Lei, Q.; Wu, J.; Fang, W. MOF Nanoparticles with Encapsulated Autophagy Inhibitor in Controlled Drug Delivery System for Antitumor. *ACS Appl. Mater. Interfaces* **2018**, *10*, 2328–2337.
- (18) Munoz-Muñoz, J. L.; Garcia-Molina, F.; Ros, E.; Tudela, J.; Garcia-Canovas, F.; Rodriguez-Lopez, J. N. PROOXIDANT AND ANTIOXIDANT ACTIVITIES OF ROSMARINIC ACID. *J. Food Biochem.* **2013**, *37*, 396–408.
- (19) Deng, Y.-T.; Chang, T.-W.; Lee, M.-S.; Lin, J.-K. Suppression of Free Fatty Acid-Induced Insulin Resistance by Phytopolyphenols in C2C12 Mouse Skeletal Muscle Cells. *J. Agric. Food Chem.* **2012**, *60*, 1059–1066.
- (20) Chen, X.; Shi, Z.; Tong, R.; Ding, S.; Wang, X.; Wu, J.; Lei, Q.; Fang, W. Derivative of Epigallocatechin-3-gallate Encapsulated in ZIF-8 with Polyethylene Glycol-Folic Acid Modification for Target and pH-Responsive Drug Release in Anticancer Research. *ACS Biomater. Sci. Eng.* **2018**, *4*, 4183–4192.
- (21) Liu, B.; Yan, W. Lipophilization of EGCG and effects on antioxidant activities. *Food Chem.* **2019**, *272*, 663–669.
- (22) Zhang, S.; Ding, S.; Yu, J.; Chen, X.; Lei, Q.; Fang, W. Antibacterial Activity, *In Vitro* Cytotoxicity, and Cell Cycle Arrest of Gemini Quaternary Ammonium Surfactants. *Langmuir* **2015**, *31*, 12161–12169.
- (23) Zhang, J.; Zhang, C.; Chen, X.; Quek, S. Y. Effect of spray drying on phenolic compounds of cranberry juice and their stability during storage. *J. Food Eng.* **2020**, *269*, 109744.
- (24) Scheffer, F. R.; Silveira, C. P.; Morais, J.; Bettini, J.; Cardoso, M. B. Tailoring Pseudo-Zwitterionic Bi-Functionalized Silica Nanoparticles: From Colloidal Stability to Biological Interactions. *Langmuir* **2020**, *36*, 10756–10763.
- (25) Arakawa, H.; Maeda, M.; Okubo, S.; Shimamura, T. Role of hydrogen peroxide in bactericidal action of catechin. *Biol. Pharm. Bull.* **2004**, *27*, 277–281.
- (26) Lecumberri, E.; Dupertuis, Y. M.; Miralbell, R.; Pichard, C. Green tea polyphenol epigallocatechin-3-gallate (EGCG) as adjuvant in cancer therapy. *Clin. Nutr.* **2013**, *32*, 894–903.
- (27) Zhang, H.; Cao, D.; Cui, W.; Ji, M.; Qian, X.; Zhong, L. Molecular bases of thioredoxin and thioredoxin reductase-mediated prooxidant actions of (–)-epigallocatechin-3-gallate. *Free Radical Biol. Med.* **2010**, *49*, 2010–2018.
- (28) Kanadzu, M.; Lu, Y.; Morimoto, K. Dual function of (–)-epigallocatechin gallate (EGCG) in healthy human lymphocytes. *Cancer Lett.* **2006**, *241*, 250–255.
- (29) Ouyang, J.; Zhu, K.; Liu, Z.; Huang, J. Prooxidant Effects of Epigallocatechin-3-Gallate in Health Benefits and Potential Adverse Effect. *Oxid. Med. Cell. Longevity* **2020**, *2020*, 9723686.
- (30) Shaikh, S.; Younis, M.; Rehman, F. U.; Jiang, H.; Wang, X. Specific Oxide Nanoclusters Enhance Intracellular Reactive Oxygen Species for Cancer-Targeted Therapy. *Langmuir* **2020**, *36*, 9472–9480.
- (31) Ji, Z.; Yin, Z.; Jia, Z.; Wei, J. Carbon Nanodots Derived from Urea and Citric Acid in Living Cells: Cellular Uptake and Antioxidation Effect. *Langmuir* **2020**, *36*, 8632–8640.
- (32) Xing, L.; Zhang, H.; Qi, R.; Tsao, R.; Mine, Y. Recent Advances in the Understanding of the Health Benefits and Molecular Mechanisms Associated with Green Tea Polyphenols. *J. Agric. Food Chem.* **2019**, *67*, 1029–1043.
- (33) Xie, H.; Xiang, C.; Li, Y.; Wang, L.; Zhang, Y.; Song, Z.; Ma, X.; Lu, X.; Lei, Q.; Fang, W. Fabrication of ovalbumin/ $\kappa$ -carrageenan complex nanoparticles as a novel carrier for curcumin delivery. *Food Hydrocolloids* **2019**, *89*, 111–121.
- (34) Ozgun, G. S.; Ozgun, E. The cytotoxic concentration of rosmarinic acid increases MG132-induced cytotoxicity, proteasome inhibition, autophagy, cellular stresses, and apoptosis in HepG2 cells. *Hum. Exp. Toxicol.* **2020**, *39*, 514–523.
- (35) Fu, J.; Hao, L.; Tian, Y.; Liu, Y.; Gu, Y.; Wu, J. miR-199a-3p is involved in estrogen-mediated autophagy through the IGF-1/mTOR pathway in osteocyte-like MLO-Y4 cells. *J. Cell. Physiol.* **2018**, *233*, 2292–2303.

(36) Xiao, X.; Wang, W.; Li, Y.; Yang, D.; Li, X.; Shen, C.; Liu, Y.; Ke, X.; Guo, S.; Guo, Z. HSP90AA1-mediated autophagy promotes drug resistance in osteosarcoma. *J. Exp. Clin. Cancer Res.* **2018**, *37*, 201.

(37) Chen, X.; Tong, R.; Liu, B.; Liu, H.; Feng, X.; Ding, S.; Lei, Q.; Tang, G.; Wu, J.; Fang, W. Duo of (–)-epigallocatechin-3-gallate and doxorubicin loaded by polydopamine coating ZIF-8 in the regulation of autophagy for chemo-photothermal synergistic therapy. *Biomater. Sci.* **2020**, *8*, 1380–1393.